Supplementary Information

Bifunctional electrocatalysts $Pr_{0.5}Sr_{0.5}Cr_{0.1}Fe_{0.9-x}Ni_xO_{3-\delta}$ (x=0.1,0.2) for HOR and ORR of a symmetric solid oxide fuel cell

Table S1. Rietveld refinement results of XRD patterns of samples.

Parameters	$PSCFN_{0.2}$ Perovskite	$PSCFN_{0.1}$ Perovskite
Space Group	*Pm*-3*m*	*Pm*-3*m*
a (Å)	3.85860	3.87139
b (Å)	3.85860	3.87139
c (Å)	3.85860	3.87139
α (º)	90	90
β (º)	90	90
γ (º)	90	90
Volume (Å^3)	57.450	58.023
R_p (%)	1.94	5.48
R_{wp} (%)	2.46	7.76
R_{exp} (%)	0.91	1.53

Table S2. Performance comparison of cells in this work and other high-performance electrolyte-supported single cells reported recently.

cathode	Electrolyte	anode	Electrolyte thickness [μm]	Temp. [ºC]	P_{max} [mW cm^{-2}]	Authors, Year
$La_{0.6}Sr_{0.4}Fe_{0.8}Co_{0.2}O_{3-\delta}$(LSCF)	$La_{0.9}Sr_{0.1}Ga_{0.8}Mg_{0.2}O_{3-\delta}$ (LSGM91)	$Sr_{1.95}Fe_{1.4}Mo_{0.5}Ni_{0.1}O_{6-\delta}$	~300	800 750 700	600 420 260	Sun et al., 2016[1]
$SrFe_{0.8}W_{0.2}O_{3-\delta}$(SFW)	$La_{0.8}Sr_{0.2}Ga_{0.8}Mg_{0.2}O_{3-\delta}$ (LSGM)	SFW	300	800 750 700	580 390 220	Zhu et al., 2020[2]
$Sr_2Ti_{0.8}Co_{0.2}FeO_{6-\delta}$ (STCF)	LSGM91	STCF	270	850 800 750	710 560 370	Niu et al., 2020[3]
$Sr_2Fe_{1.4}Mo_{0.5}Nb_{0.1}O_{6-\delta}$ (SFNNb)	$La_{0.8}Sr_{0.2}Ga_{0.8}{}_3Mg_{0.17}O_{3-\delta}$	SFMNb	243	800 750 700	540 350 230	Guo et al., 2019[4]

$Gd_{0.6}5Sr_{0.35}(Co_{0.25}Fe_{0.75})_{0.9}Ce_{0.1}O_{3-\delta}$ (Ce-GSCF)	$Gd_{0.2}Ce_{0.8}O_{2-\delta}$ (GDC)	Ce-GSCF	300	700 650 600	224 175 91	Tian et al., 2020[5]
$BaZr_{0.1}Co_{0.4}Fe_{0.4}Y_{0.1}O_3$ (BZCFY) - $Sm_{0.2}Ce_{0.8}O_2$ (SDC)	$BaZr_{0.2}Ce_{0.7}Y_{0.1}O_3$	SDC-BZCFY	480	650 600	115 74	Fan et al., 2018[6]
$NdBaCo_{2/3}Fe_{2/3}Cu_{2/3}O_{5+\delta}$	LSGM91	$Sr_2Fe_{0.5}Mo_{0.5}TiO_{6-\delta}$	200	800 750 700	730 550 340	Niu et al., 2018[7]
$Sm_{0.70}Sr_{0.20}Fe_{0.8}Ti_{0.15}Ru_{0.05}O_{3-\delta}$ (SSFTR7020)	$Sm_{0.2}Ce_{0.8}O_{1.9}$ (SDC)	SSFTR7020	600	800 750 700	337 240 125	Bai et al., 2020[8]
$Ba_{0.5}Sr_{0.5}Co_{0.8}Fe_{0.2}O_{3-\delta}$ (BSCF)	$La_{0.8}Sr_{0.2}Ga_{0.83}Mg_{0.17}O_{3-\delta}$	$Sr_2Fe_{1.5}Mo_{0.5}O_{6-\delta}$(SFM)	300	850 800 750	620 530 460	Wang et al., 2014[9]
$La_{0.25}Sr_{2.75}FeNiO_{7-\delta}$ (LSFN) - $Gd_{0.1}Ce_{0.9}O_{2-\delta}$ (GDC)	YSZ	LSFN-GDC	300	800 750 700	232 128 73	Lin et al., 2021[10]
$(SmBa)_{0.9}Mn_{1.8}Co_{0.2}O_{5+\delta}$ (SBMCo)	$La_{0.8}Sr_{0.2}Ga_{0.8}Mg_{0.2}O_{3-\delta}$ (LSGM)	SBMCo	300	850 800 750	560 426 320	Zhao et al., 2023[11]
$Ba_{0.9}La_{0.1}Co_{0.7}Fe_{0.2}Nb_{0.1}O_{3-\delta}$ (BLCFN)	SDC	BLCFN	300	750	362	Ding et al., 2022[12]
$PSCFN_{0.1}$	LSGM	re-$PSCFN_{0.1}$		850 800 750	768 570 412	**This work**
$PSCFN_{0.2}$	LSGM	re-$PSCFN_{0.2}$		850 800 750	851 623 476	**This work**

Table S3. Fitting parameters for the impedance spectra of the $PSCFN_x$/LSGM/ $PSCFN_x$ symmetric half-cells at 700 ºC-850 ºC.

Electrode	Atmosphere	Temperature (ºC)	R_0 ($\Omega \cdot cm^2$)	R_1 ($\Omega \cdot cm^2$)	R_2 ($\Omega \cdot cm^2$)	R_3 ($\Omega \cdot cm^2$)
$PSCFN_{0.1}$	H_2	850	0.20	0.07	0.26	1.86
		800	0.27	0.19	0.21	2.04

		750	0.39	0.13	0.37	2.40
		700	0.58	0.05	0.68	2.87
		850	0.19	-	0.06	0.03
		800	0.27	0.03	0.07	0.09
	air					
		750	0.38	0.03	0.13	0.18
		700	0.56	0.08	0.24	0.34
		850	0.19	0.03	0.10	0.79
		800	0.26	0.12	0.18	0.98
	H_2					
		750	0.37	0.08	0.42	1.37
		700	0.54	0.04	0.81	1.76
$PSCFN_{0.2}$						
		850	0.19	-	0.02	0.03
		800	0.27	-	0.04	0.05
	air					
		750	0.37	0.04	0.05	0.06
		700	0.57	0.07	0.08	0.12

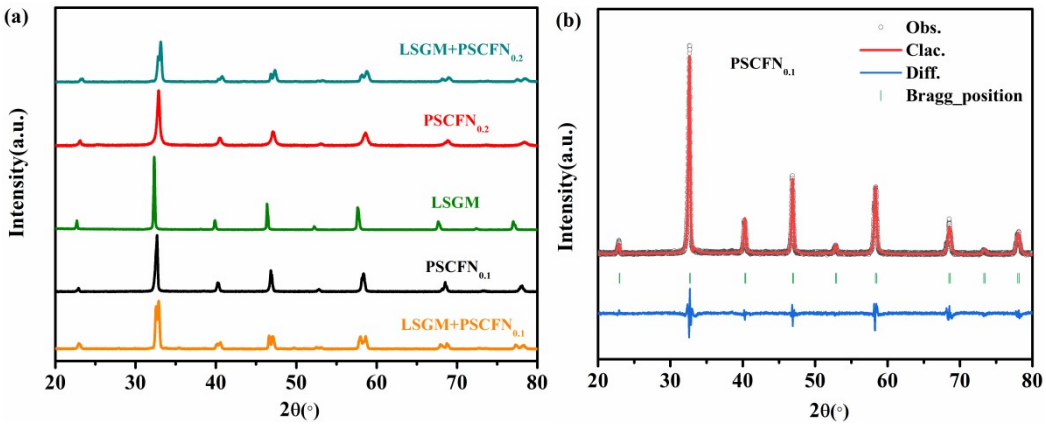

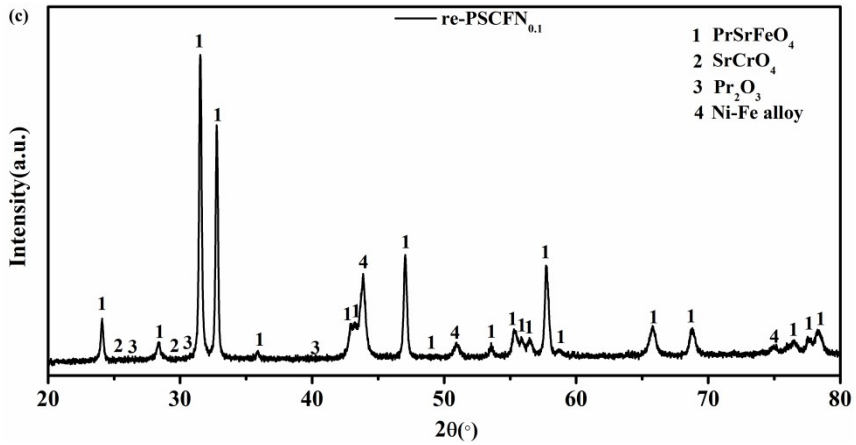

Figure S1 (a) XRD patterns of $PSCFN_x$, LSGM and calcined $PSCFN_x$-LSGM mixture (1:1 mass ratio), re-$PSCFN_x$: reduced at 850 °C for 10 h in 5% H_2/Ar, (b) Rietveld XRD refinement of the $PSCFN_{0.1}$ powder, (c) re-$PSCFN_{0.1}$ powder.

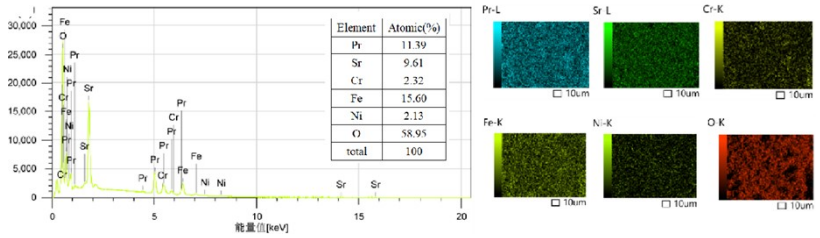

Figure S2 SEM-EDS mappings of the $PSCFN_{0.2}$ powder

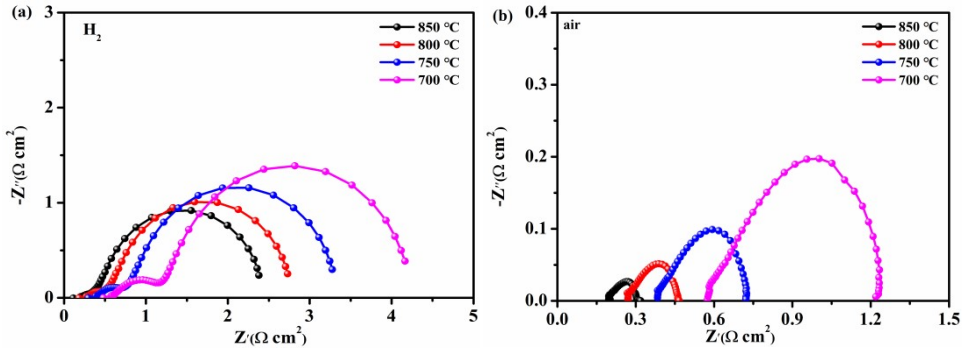

Figure S3 The electrochemical impedance of $PSCFN_{0.1}$ electrode in the symmetrical half-cell in H_2 and air.

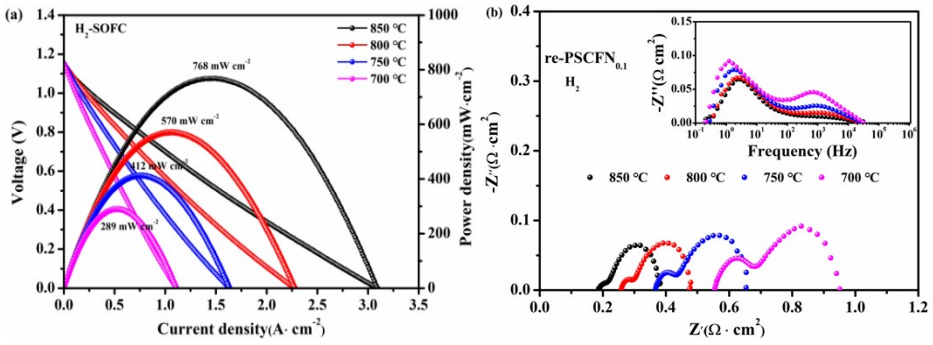

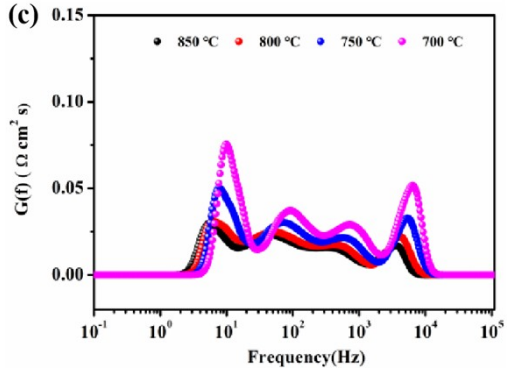

Figure S4 (a) Typical I-V-P curves, (b) Temperature dependence of the polarization resistance (R_p), (c) DRT analysis of the single cells with the anode (re-PSCFN$_{0.1}$) fueled with H_2.

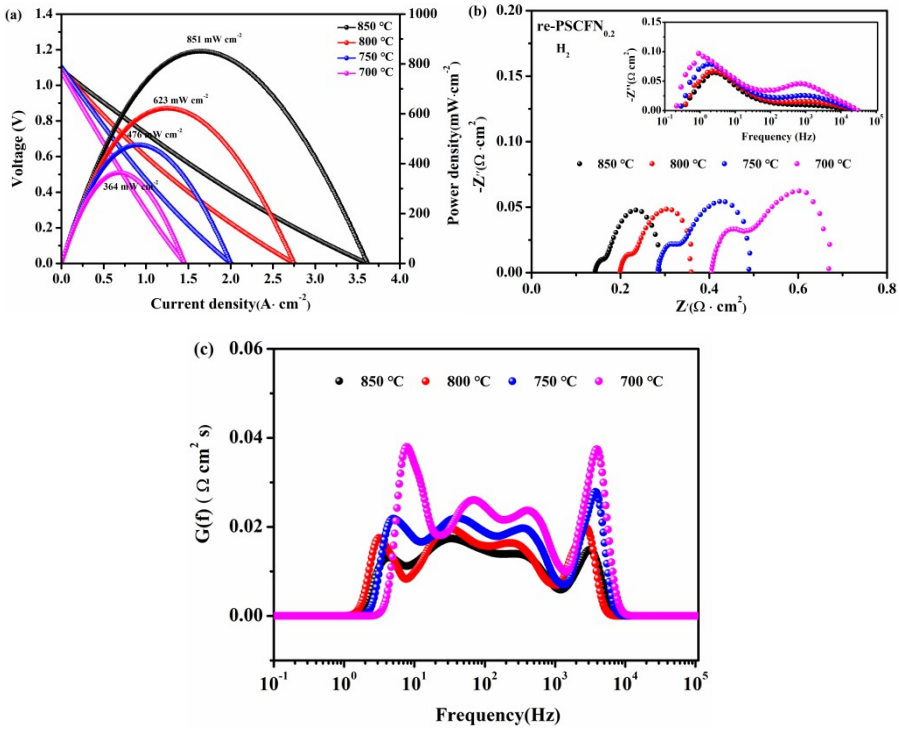

Figure S5 (a) Typical I-V-P curves, (b) Temperature dependence of the polarization resistance (R_p), (c) DRT analysis of the single cells with the anode (re-PSCFN$_{0.2}$) fueled with H_2.

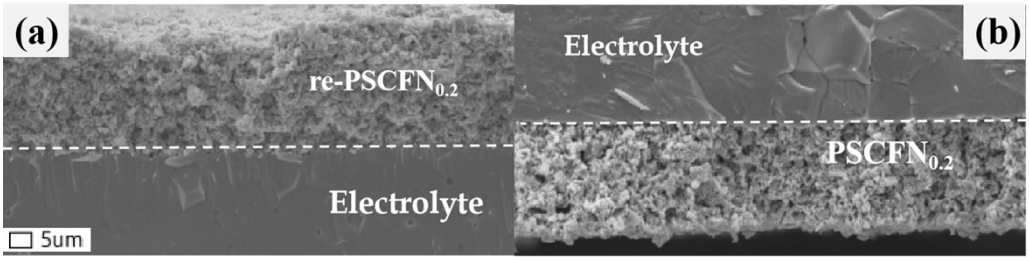

Figure S6 SEM images of the LSGM-supported single cell with a configuration of an re-PSCFN$_{0.2}$ anode, LSGM electrolyte, and PSCFN$_{0.2}$ air electrode.

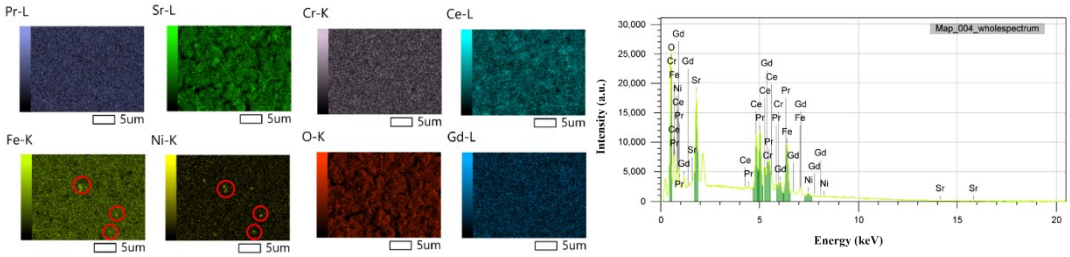

Figure S7 SEM-EDS mapping images of the re-PSCFN$_{0.2}$ anode after the stability tests. The red circles represent Ni-Fe alloys.

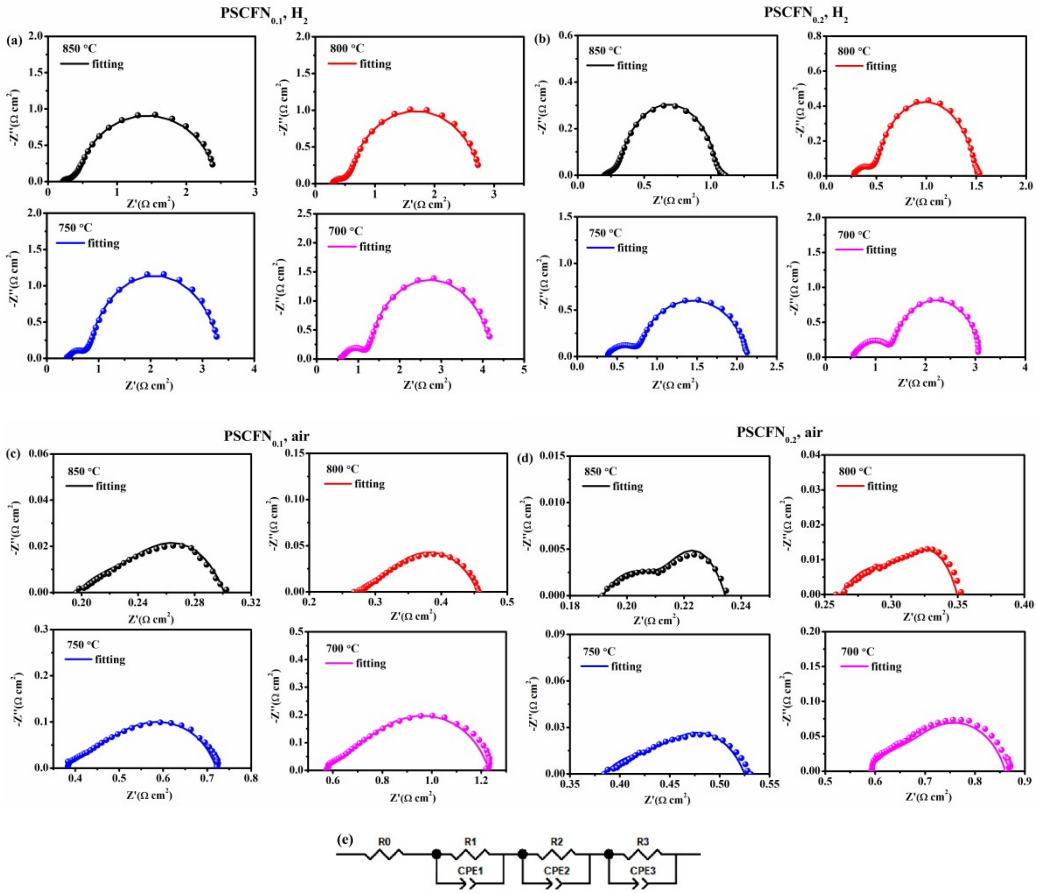

Figure S8 (a-d) Experimental and fitting results of impedance spectra for PSCFN$_x$/LSGM/ PSCFN$_x$ symmetric half-cells at 700 ºC-850 ºC, (e) equivalent circuit for the impedance spectra.

References in Table S2

[1] Jie Feng, Jinshuo Qiao, Wenyi Wang, Zhenhua Wang, Wang Sun, Kening Sun, Development and performance of anode material based on A-site deficient $Sr_{2-x}Fe_{1.4}Ni_{0.1}Mo_{0.5}O_{6-\delta}$ perovskites for solid oxide fuel cells, Electrochimica Acta 215 (2016) 592-599.

[2] Yanxin Cao, Zhiwen Zhu, Yujun Zhao, Wen Zhao, Zhaoling Wei, Tong Liu, Development of tungsten stabilized $SrFe0_{.8}W_{0.2}O_{3-\delta}$ material as novel symmetrical electrode for solid oxide fuel

cells, Journal of Power Sources 455 (2020) 227951-227962.

[3] Bingbing Niu, Chunling Lu, Wendi Yi, Shijing Luo, Xiangnan Li, Xiongwei Zhong, Xingzhong Zhao, Baomin Xu, *In-situ* growth of nanoparticles-decorated double perovskite electrode materials for symmetrical solid oxide cells, Applied Catalysis B: Environmental 270 (2020) 118842-118857.

[4] Manli Gou, Rongzheng Ren, Wang Sun, Chunming Xu, Xingguang Meng, Zhenhua Wang, Jinshuo Qiao, Kening Sun, Nb-doped $Sr_2Fe_{1.5}Mo_{0.5}O_{6-\delta}$ electrode with enhanced stability and electrochemical performance for symmetrical solid oxide fuel cells, Ceramics International 45 (2019) 15696-15704.

[5] Kai Song, Zhipeng Yu, Xiaoyan Luo, Shiyue Zhu, Yang Yang, Quan Yang, Dong Tian, Xiaoyong Lu, Yanzhi Ding, Yonghong Chen, Bin Lin, A simple Ce-doping strategy to enhance stability of hybrid symmetrical electrode for solid oxide fuel cells, International Journal of Hydrogen Energy 45 (2020) 29259-29270.

[6] Yingqin Yu, Lixiang Yu, Kang Shao, Yihang Li, Kristina Maliutina, Wenxiang Yuan, Qixing Wu, Liangdong Fan, $BaZr_{0.1}Co_{0.4}Fe_{0.4}Y_{0.1}O_3$-SDC composite as quasi-symmetrical electrode for proton conducting solid oxide fuel cells, Ceramics International 46 (2020) 11811-11818.

[7] Bingbing Niu, Fangjun Jin, Xin Yang, Tao Feng, Tianmin He, Resisting coking and sulfur poisoning of double perovskite $Sr_2TiFe_{0.5}Mo_{0.5}O_{6-\delta}$ anode material for solid oxide fuel cells, International Journal of Hydrogen Energy 43 (2018) 3280-3290.

[8] Weiwei Fan, Zhu Sun, Yu Bai, Kai Wu, Jun Zhou, Yonghong Cheng, *In situ* growth of nanoparticles in A-site deficient ferrite perovskite as an advanced electrode for symmetrical solid oxide fuel cells, Journal of Power Sources 456 (2020) 228000-228011.

[9] Y. Wang, P. Li, H. Li, Y. Zhao, Y. Li, Synthesis and Enhanced Electrochemical Performance of Sm-Doped $Sr_2Fe_{1.5}Mo_{0.5}O_6$, Fuel Cells 14 (2014) 973-978.

[10] Yihan Ling, Lu Liu, Shijie Zhou, Yang Yang, Hui Zhu, Hui Chen, M.H. Paydar, Shaorong Wang, Leveraging in-situ formation of Ni-Fe nanoparticles to promote the catalytic performance of Ruddlesden-Popper based electrode for symmetrical solid oxide fuel cells, International Journal of Hydrogen Energy 46 (2021) 27149-27155.

[11] Yang Zhang, Hailei Zhao, Min Zhang, Zhihong Du, Wanbing Guan, Subhash C. Singhal, Konrad Świerczek, Boosting the Electrode Reaction Kinetics of SSOFCs by the Synergistic Effect of Nanoparticle Codecoration on Both the Cathode and Anode, Chemistry Materials 35

*(*2023)499-510.

[12] Xinghong Zhou, Mingze Li, Weimin Yang, Haibo Hu, Jun Li, Yi Lu, Xiaoyu Wang, Xifeng Ding, Efficient and stable symmetrical solid oxide fuel cell via A-site non-stoichiometry, Electrochimica Acta 425 (2022) 140697-140708.